Various characteristics of a waveguide-mode free-electron laser using a long-pulse relativistic electron beam

Y. Kawamura
The Institute of Physical and Chemical Research (RIKEN), Wako, Saitama 351-01, Japan

B. C. Lee
*Department of Physics, Korea Advanced Institute of Science and Technology, P.O. Box 8, Cheongryang, Seoul, South Korea**

M. Kawai
Department of Physics, Faculty of Science, Tokai University, Hiratuka-shi, Kanagawa 259-12, Japan†

K. Toyoda
The Institute of Physical and Chemical Research (RIKEN), Wako, Saitama 351-01, Japan
(Received 30 October 1992)

In this paper, various characteristics, such as the small-signal gain, oscillation threshold, and self-mode-locked oscillation behavior, of a waveguide-mode free-electron laser using a long-pulse relativistic electron beam are described. Analysis of the wave forms of the output radiation and the modulation of the electron beams was carried out in order to demonstrate the existence of coupling between different oscillation branches through the electron beams.

PACS number(s): 41.60.Cr, 42.60.Fc

I. INTRODUCTION

Free-electron lasers are classified into two categories. One is the Compton-type free-electron laser, which uses high-energy and low-current electron beams and consequently generates short-wavelength radiation [1–3]. The other is the Raman-type free-electron laser, which uses relatively low-energy and high-current electron beams, and operates at relatively long wavelengths [4–12]. In the latter case, a waveguide is necessary to compose a cavity resonator to confine the electromagnetic radiation until it exceeds the threshold of oscillations. The use of a waveguide makes the interaction between the electron beam and the electromagnetic radiation in the cavity resonator complex compared to that in the case of Compton-type free-electron lasers. This makes oscillation possible not only at different longitudinal cavity modes but also at different oscillation branches, which are called the upper and lower branches of the waveguide-mode free-electron laser oscillations.

Among these Raman-type free-electron lasers, periodical pulse trains have been observed in the wave form of the output power, and some of them were recognized as self-mode-locked oscillations [5,9–11]. Recently, active mode-locked oscillation of free-electron lasers has been reported, and the limitation on shortening of the pulse width was shown to be determined by the slippage time between the electron beam and the electromagnetic radiation in the cavity resonator [12].

In this paper, various characteristics, such as a small-signal gain, oscillation thresholds, and self-mode-locked oscillation behaviors, of a waveguide-mode free-electron laser are reported. The pulse-train intervals of the self-mode-locked oscillation wave forms for various experiment parameters were analyzed in order to prove the existence of coupling between the different oscillation branches through electron beams.

II. EXPERIMENTAL APPARATUS

The experimental setup is shown in Fig. 1. An electron beam from a plasma cathode [5,13] is accelerated electrostatically and introduced into a waveguide cavity resonator through a small hole at the corner of the waveguide oscillator. The acceleration voltage can be varied from 500 to 570 keV. The time constant of the voltage decay is about 20 μs; thus the voltage change is about 1% for 200 ns. The wave form of the electron-beam current is not reproducible, and the average current was varied from about 10 to 25 A. The energy spread of this electron beam ($\Delta E/E$) has not been measured, but it is estimated to be on the order of 0.1%, judging from the characteristics of the cold relativistic electron-beam source [13], which is the origin of the electron beam used in this experiment. The number of periods of the wiggler is 20. The adiabatic region consists of 2.5 pitches, in which the magnetic-field strength of the wiggler (B_w) gradually increases. The pitch of the wiggler period (λ_w) is 5 cm. The waveguide resonator is composed of a straight waveguide tube having two corners on both sides. Two mirrors made of flat copper plates are attached on both sides of the corners. One of them has a coupling hole of 3-mm diameter to extract output power. The dimensions of the waveguide and the length between mirrors along the axis of the waveguide are 2.29×1.02 cm^2 and 122 cm, respectively. A longitudinal magnetic field (B_g) of 2.1 kG is applied in order to guide the electron beam along the axis of the waveguide.

Output power of the free-electron laser oscillation is introduced into a crystal detector (1N26) through a tapered

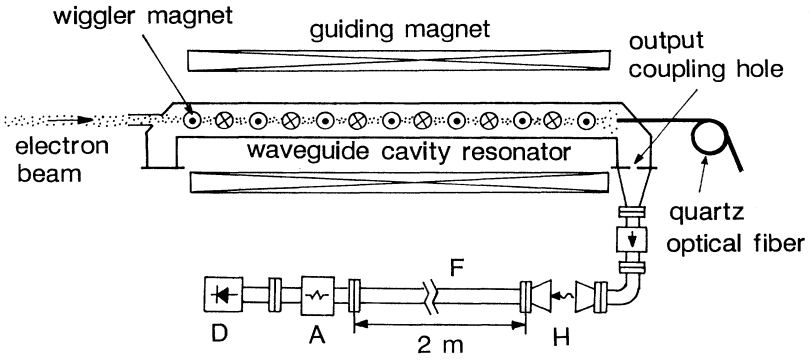

FIG. 1. Experimental setup of the waveguide-mode free-electron laser. *I*: isolator; *H*: microwave horns; *A*: attenuator; *D*: microwave detector (1N26 crystal diode); *F*: high-pass filter.

waveguide and then through a waveguide operating as a high-pass filter for the output signal of the free-electron laser oscillation. The cutoff frequency of this waveguide is 21.1 GHz. The length is 2 m, which is long enough to enable the waveguide to operate as a high-pass filter for signals higher than the cutoff frequency. The signal is attenuated at a rate of 70 dB in order to obtain linear operation characteristics of the crystal detection. A pair of microwave horns was used for the electrical insulation between the cavity resonator and the signal detection system. The step response of the signal diagnostic system, which is determined by the oscilloscope and the signal cable, was measured to be 3.9 ns. The impulse response, which is equal to the step response for a linear-response system, is estimated to be 3.9 ns. The electron-beam density on the axis of the waveguide after transmission through the waveguide cavity resonator, where the free-electron laser interactions took place, was measured using Čerenkov radiation of the quartz optical fiber irradiated by the electron beam. The spectral component of 410±5 nm of the Čerenkov radiation was measured by a photomultiplier to the wave-form distortion due to the dispersions in the optical fiber.

In case of the gain measurement, microwave power of 32 GHz was injected as a probe signal from one side of the waveguide cavity resonator, and the electron-beam current was adjusted to remain within the range of 10±1 A. The behavior of the electron-beam motion in the wiggler and the small-signal gain were measured using low-current electron beams in previous experiments [14,15].

III. OSCILLATION MODE ANALYSIS

The dispersion relation of the electromagnetic radiation in the waveguide is given by

$$(2\pi f)^2=(ck)^2+(2\pi f_c)^2 , \quad (1)$$

where f and k are the angular frequency of the electromagnetic radiation and the wave number in the waveguide, respectively, c is the light velocity, and f_c is the cutoff frequency of the TE_{10} waveguide mode, which was calculated to be 6.55 GHz. The dispersion relation for the space-charge wave, which is produced by the wiggling electron beam in the wiggler, is given by

$$2\pi f=\beta c(k+k_w) , \quad (2)$$

where f and k are the frequency and the wave number, respectively, β is defined by $\beta=v/c$, where v is the parallel velocity component of the electron beam, and k_w is the wave number of the wiggler and is defined by $k_w=2\pi/\lambda_w$, where λ_w is the pitch length of the wiggler. Equations (1) and (2) are drawn in Fig. 2. The experimental parameters of $E=526$ kV, $B_w=0.36$ kG, and $B_g=2.1$ kG are used to draw Fig. 2.

Since the operation of the waveguide-mode free-electron laser is defined as the coupling between the space-charge wave and the waveguide mode, it is determined from the solutions to Eqs. (1) and (2). A pair of solutions is obtained at the cross points in Fig. 2, which are defined by the oscillation frequency of the upper branch (f_u) and that of the lower branch (f_l). For the experimental parameters chosen in this experiment, these are calculated to be $f_u=34.4$ GHz and $f_l=6.81$ GHz.

IV. EXPERIMENTAL RESULTS

A. Gain measurements

Small-signal gains of this free-electron laser oscillator were measured by injecting a microwave signal of 32

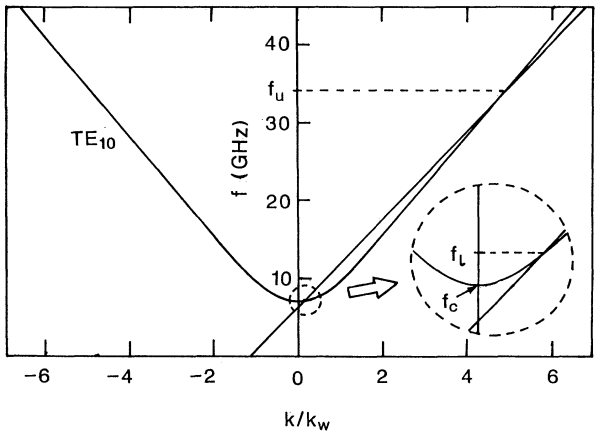

FIG. 2. Dispersion relations of the TE_{10} mode in the waveguide cavity resonator and a space-charge wave. f_u and f_e are the frequency of the upper-branch and lower-branch oscillations, respectively. f_c is the cutoff frequency of the waveguide cavity resonator. Horizontal scale is normalized by the wave number of the wiggler.

GHz from one side of the waveguide cavity resonator. In this measurement, the electron-beam current was adjusted to remain within the range of 10±1 A. Since the acceleration voltage varies continuously, it is possible to obtain gain spectra with respect to the electron-beam energy in a single shot.

Figure 3 shows a typical experimental result of the small-signal gain measurement. Here (a) shows the amplified (or absorbed) signal of the input microwave. Arrows in the figure show the amplification and absorption. Figures 3(b) and 3(c) show the acceleration voltage and the electron-beam current, respectively. The arrow in 3(b) represents the resonance energy of the electron beam.

Figure 4 shows the small-signal gain coefficient per ampere as a function of the wiggler magnetic-field strength. The solid line in the figure represents the best-fit line for these data. For comparison, the small-signal gain coefficient for the same microwave frequency in the case of the Compton-regime operation obtained by the same facility is shown as a dashed line in the figure. This result was obtained in a previous paper, using a low-current electron beam [14]. The dashed line is the best-fit line for the measured small gain of the Compton-regime operation. Comparing the experimental results with the dashed line, it is easily found that the free-electron laser operation obtained in this experiment is not in the Compton regime. The discrepancy between these two cases is considered to be mainly due to the difference in the electron-beam current, and shows that this experimental system operates in a Raman regime.

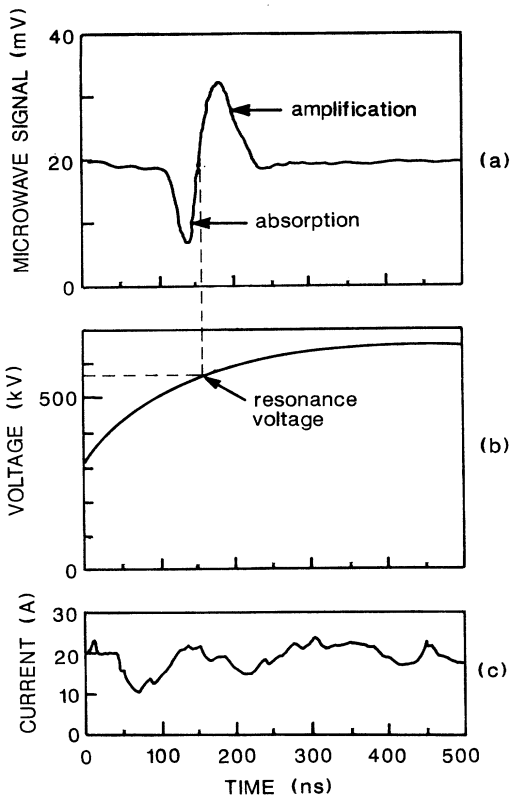

FIG. 3. Typical wave forms of the amplified (or absorbed) microwave signal (a), acceleration voltage of the electron beam (b), and the electron-beam current (c).

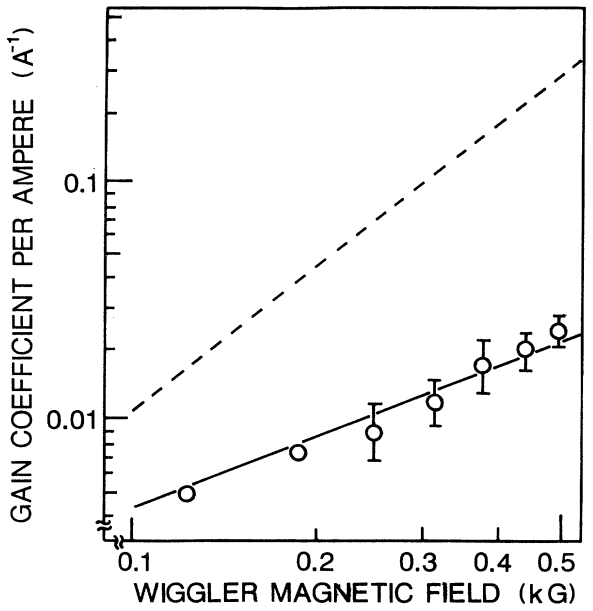

FIG. 4. Gain coefficient per ampere for the 32-GHz microwave signal. Total electron-beam current was adjusted to 10±1 A.

B. Oscillation threshold

Figure 5 shows typical wave forms of the output power of the free-electron laser. Figure 5(a) shows a periodically modulated wave form, which appears occasionally and is considered to be the self-mode-locked oscillation of a free-electron laser [5,9–11]. Figure 5(b) shows a randomly modulated wave form, which is considered to be due to interference between a few longitudinal oscillation modes of the cavity resonator. This signal is the radiation of the upper-branch oscillations. Since the theoretical value of the lower-branch oscillation frequency f_l is lower than the cutoff frequency of the waveguide operating as a high-pass filter, it is not detectable.

Figure 6 shows the oscillation thresholds as a function of the wiggler magnetic-field strength and the electron-

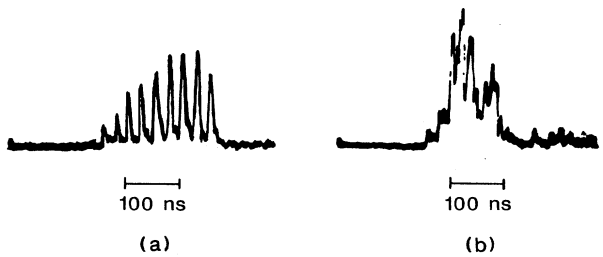

FIG. 5. Typical wave forms of the output of the waveguide-mode free-electron laser. (a) is a periodically modulated wave form, which appears occasionally and is considered to be a self-mode-locked oscillation. (b) is a randomly modulated wave form, which is considered to appear due to the interference between a few longitudinal modes of the cavity resonator.

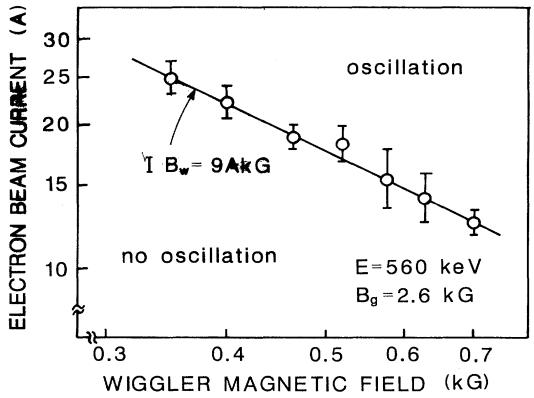

FIG. 6. Threshold behavior of the free-electron laser oscillations. Error bars in the figure represent the region of the electron-beam current where the oscillation occurred occasionally. Therefore the solid line in the figure represents the threshold of the oscillations.

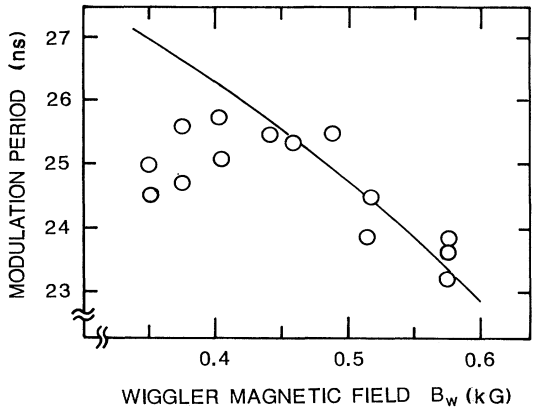

FIG. 7. Pulse-train periods of the upper-branch oscillation as a function of the wiggler magnetic field B_w. The energy of the electron beam $E=524$ keV. The solid line is the theoretical calculations of the round-trip time in the cavity resonator using the group velocity of the lower branch.

beam current. The error bars in the figure represent the region of the electron-beam current in which the oscillations occasionally occurred. For a fixed wiggler magnetic-field strength, the oscillations did not occur when the electron-beam current fell short of the bottom edges of the error bars. On the contrary, the oscillation always occurred when the electron-beam current was higher than the upper edge of the error bars. Consequently, the solid line in the figure represents the threshold of oscillations. This is expressed by $IB_w=9$ A kG and is linearly proportional to the wiggler magnetic-field strength B_w, which is a typical characteristic of a Raman-type free-electron laser. It was reported that the small-signal gain of this experimental setup was proportional to the square of B_w for the electron-beam current of 1 A [14], which is a typical characteristic of a Compton-type free-electron laser. This discrepancy between these two cases can be explained by the difference in the electron-beam current and shows that this experimental system operates in the Raman regime.

C. Periodicities of pulse trains

Figures 7 and 8 show the pulse-train period of the output wave form as a function of the wiggler magnetic field B_w and the energy of the electron beam E, respectively. In the waveguide-mode oscillation, the pulse-train period of the mode-locked oscillation corresponds to the round-trip time of the electromagnetic radiation in the cavity with a group velocity v_g [5]. The solid lines in Figs. 7 and 8 are the theoretical calculations of the round-trip time of the cavity resonator using the group velocity of the lower branch. For wide ranges of B_w and E, the experimental data were in good agreement with the theoretical calculations. The theoretical calculation of the round-trip time for the upper branch was about 8.3 ns in this experiment, which is approximately one-third that for the lower branch, and was not in agreement with the experimental results shown in Figs. 7 and 8.

The discrepancies between the theoretical and the experimental vales for smaller B_w ($B_w<0.45$ kG) and higher E ($E>530$ keV) are considered to be due to the fact that f_l approaches the cutoff frequency of the waveguide cavity resonator, and the loss of the cavity increases abruptly in these experimental parameter regions.

The interesting point of these experimental results is the fact that the wave form of the upper branch is modulated periodically with the period equal to the self-mode-locked oscillation of the lower branch. These experimental results show that coupling exists between the electromagnetic waves of the upper-branch and the lower-branch oscillations in the waveguide cavity resonator. It is natural to consider that the intermediate of this coupling is the electron beams.

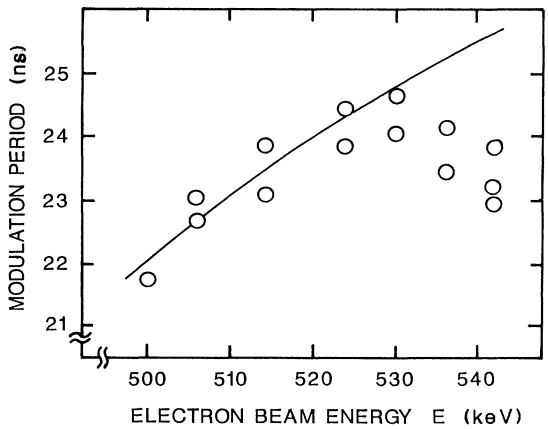

FIG. 8. Pulse-train periods of the upper-branch oscillation as a function of the energy of the electron beam (E). The wiggler magnetic field $B_w=0.54$ kG. The solid line is the theoretical calculation of the round-trip time in the cavity resonator using the group velocity of the lower branch.

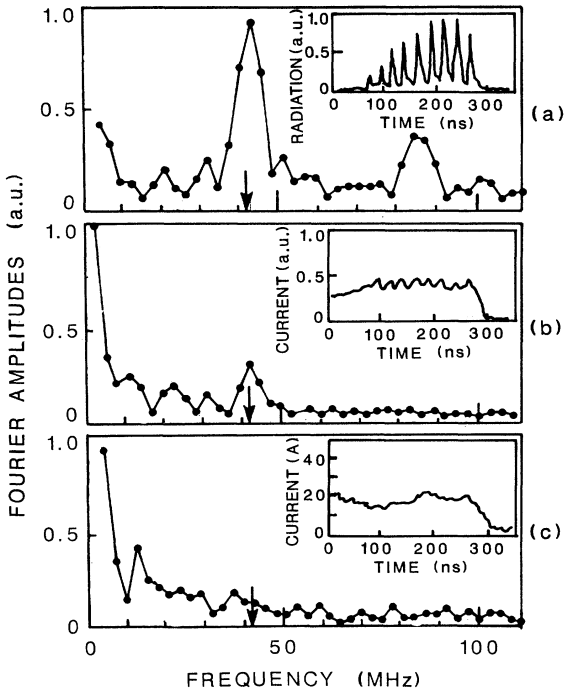

FIG. 9. Fourier power spectra of the oscillation wave form (a), the current wave form of the electron beam after interaction with the wiggler (b), and before interaction with the wiggler (c).

D. Transverse density modulation of the electron beam

In this experimental setup, the relative value of the current density of the electron beam can be measured at the exit of the waveguide. It is expected that this value changes when the electron beam experiences density modulation in the transverse direction.

In order to demonstrate the existence of interactions between the electron beam and the electromagnetic radiation of the lower-branch oscillations, Fourier power spectra of the oscillation wave form having periodical pulse trains were compared with those of the wave forms of the electron-beam current density measured on the axis of the waveguide after interaction with the wiggler and the total current measured before interaction with the wiggler. These are shown in Fig. 9. In the Fourier power spectra of the current density of the electron beam measured on the axis of the waveguide, a peak corresponding to the frequency of periodicity of the output wave form can be clearly seen. On the other hand, the corresponding peak cannot be seen in the Fourier power spectra of the total current wave form of the electron beam, which was measured at the entrance of the waveguide. These experimental results indicate the existence of the density modulation of the electron beam in the transverse direction by the electromagnetic radiation of the lower-branch oscillation.

V. DISCUSSION

A possible explanation for the mechanism of the coupling between the upper and the lower oscillation branches through the electron beams is discussed below.

Because of the high gain and high Q value of the cavity of the lower branch, oscillations of the lower branch can be easily initiated in the waveguide cavity resonator, but cannot be extracted from the cavity due to the small coupling hole. When self-mode-locked oscillation of the lower branch occurs, the interaction between the electron beam and the electromagnetic radiation of the lower branch is the strongest at the peak of the mode-locked wave form. Bunching of the electron beam occurs in the region where the interaction takes place. In this bunched region of the electron beam, it is difficult for the electron beam to have a gain in the upper branch, because the wavelength in the waveguide of the lower-branch oscillation is about 18 times larger than that of the upper-branch oscillation. On the contrary, in the region between two adjacent peaks of the mode-locked oscillations, the interaction between the electromagnetic radiation of the lower branch and the electron beam is weak. At the center of two adjacent peaks of the mode-locked oscillation, the strength of the electromagnetic field becomes zero and bunching of the electron beam by the lower-branch oscillation no longer occurs. Therefore it is easier for the upper branch to have the gain in this region compared with the region where the electron beam is already bunched by the periods of the wavelength of the lower-branch oscillation. Consequently, the gain for the upper branch is modulated periodically by the period of the mode-locked oscillation of the lower branch. This temporal gain modulation of the upper branch, which is considered to be caused by the self-mode-locked oscillation on the lower branch, is one of the possible explanations for the phenomenon observed in this experiment.

In this experiment, the round-trip time for the lower-branch oscillation happened to be an integral multiple of that for the upper-branch oscillation. Therefore it is possible to consider that the electromagnetic radiation of the upper-branch oscillation obtains a gain every three round-trips in the cavity resonator without slippage. This condition is essential for growth of the self-mode-locked oscillations in the upper branch.

VI. CONCLUSIONS

In conclusion, various characteristics, such as the small-signal gain, oscillation threshold, and self-mode-locked oscillation behavior, of a waveguide-mode free-electron laser using a long-pulse relativistic electron beam have been described. Through analysis of the periodicities of the self-mode-locked oscillation waveforms, coupling between different oscillation branches of a waveguide-mode free-electron laser was found. It was observed that the wave form of the upper-branch oscillation of a waveguide-mode free-electron laser was modulated by the period of the mode-locked oscillation of the lower-branch oscillation over a wide range of operation parameters. This phenomenon was explained to be the temporally periodical modulation of the gain of the upper branch by the electromagnetic radiation of the lower-branch oscillation through the electron beam.

*Present address: Korea Atomic Energy Research Institute, P.O. Box 7, Daeduk-Danji, Taejon 305-606, Korea.
†Present address: Kawasaki Heavy Industries. Ltd., Kawasaki-cho, Akasi 637, Japan.

[1] L. R. Elias, W. M. Fairbank, J. M. J. Madey, H. A. Schwettman, and T. I. Smith, Phys. Rev. Lett. **36**, 717 (1976).
[2] D. A. G. Deacon, L. R. Elias, J. M. J. Madey, G. J. Ramian, H. A. Schwettman, and T. I. Smith, Phys. Rev. Lett. **38**, 892 (1977).
[3] M. Billardon, P. Elleaume, J. M. Ortega, C. Bazin, M. Bargher, M. Velghe, and Y. Petroff, Phys. Rev. Lett. **51**, 1652 (1983).
[4] S. H. Gold, W. M. Black, V. L. Granatstein, and A. K. Kinkead, Appl. Phys. Lett. **43**, 922 (1983).
[5] Y. Kawamura, K. Toyoda, and M. Kawai, Appl. Phys. Lett. **51**, 795 (1987).
[6] N. Ohigashi, M. Morita, K. Mima, S. Miyamoto, K. Imasaki, S. Kuruma, S. Nakai, C. Yamanaka, T. Taguchi, and A. Murai, Appl. Phys. Lett. **50**, 304 (1987).
[7] R. J. Harvey and F. A. Dolezal, Appl. Phys. Lett. **53**, 1150 (1988).
[8] J. Fajans, G. Bekefi, Y. Z. Yin, and B. Lax, Phys. Rev. Lett. **53**, 246 (1984).
[9] J. Masud, T. C. Marshall, S. P. Schlesinger, and F. G. Yee, Phys. Rev. Lett. **56**, 1567 (1986).
[10] E. Jerby, G. Bekefi, and J. S. Wurtele, Phys. Rev. Lett. **66**, 2068 (1991).
[11] Y. Kawamura, B. C. Lee, M. Kawai, and K. Toyoda, Phys. Rev. Lett. **67**, 832 (1991).
[12] E. Jerby, G. Bekefi, and T. Hara, Nucl. Instrum. Methods **A318**, 114 (1992).
[13] M. Kawai, Y. Kawamura, and K. Toyoda, J. Appl. Phys. **66**, 2789 (1989).
[14] B. C. Lee, Y. Kawamura, K. Toyoda, M. Kawai, and S. S. Lee, Rev. Laser Eng. **18**, 27 (1990).
[15] B. C. Lee, Y. Kawamura, K. Toyoda, M. Kawai, and S. S. Lee, Appl. Phys. Lett. **56**, 703 (1990).